Topological characterization of fractional quantum Hall ground states from microscopic Hamiltonians: Supplementary Material

Michael P. Zaletel,[1] Roger S. K. Mong,[1,2] and Frank Pollmann[3]

[1] *Department of Physics, University of California, Berkeley, California 94720, USA*
[2] *Department of Physics, California Institute of Technology, Pasadena, California 91125, USA*
[3] *Max-Planck-Institut für Physik komplexer Systeme, 01187 Dresden, Germany*

CONTENTS

I. ORBITAL n AND BOND $\bar{n}$ NOTATIONS

In the subsequent analysis, sites are labeled by n, and bonds by $\bar{n}$. The labels n are understood to take on a numerical value indicating the location of the orbital, in units of $\frac{2\pi\ell_B^2}{L}$. As will be discussed in Eq. (28), when a flux Φ_x threads through the cylinder, $n \in \mathbb{Z} + \frac{\Phi_x}{2\pi}$. We let $\bar{n}$ take on a numerical value which is the average of the site locations to the bond's left and right, i.e. $\bar{n} \in \mathbb{Z} + \frac{\Phi_x+\pi}{2\pi}$. For example, the bond between sites $n = 0$ and $n = 1$ is labeled by $\bar{n} = \frac{1}{2}$.

II. SYMMETRY PROPERTIES OF QUANTUM HALL iMPS

As the symmetry properties of MPS are a crucial part of the details that follow, we present the symmetries of quantum Hall systems on a cylinder, a review of U(1) symmetry conservation for MPS, and elaborate on the $\langle\overline{Q}\rangle$, $\langle\langle\overline{Q}\rangle\rangle$ notation.

A. Conserved quantities of the infinite cylinder

In addition to the conservation of number, it is essential to implement conservation of momentum (also called 'center of mass'), both because of the tremendous reduction in numerical effort and for the ability to label the entanglement

spectrum by momentum. At filling factor ν, we define the charges (C, K) to be

$$\hat{C} = \sum_n \hat{C}_n, \qquad \hat{C}_n = \hat{N}_n - \nu \qquad \text{(particle number)}, \tag{1a}$$

$$\hat{K} = \sum_n \hat{K}_n, \qquad \hat{K}_n = n(\hat{N}_n - \nu) \qquad \text{(momentum)}, \tag{1b}$$

where $\hat{N}_n$ is the on-site number operator. Unlike the charge C, the momentum K is peculiar as it behaves nontrivially under a translation by n sites, $\hat{T}_n$,

$$\hat{T}_{-n}\hat{K}\hat{T}_n = \hat{K} + n\hat{C} \tag{2}$$

which must be accounted for when conserving the two charges in the DMRG algorithm. If the state has a unit cell of M, the *matrices* of the MPS are periodic in M; however, due to Eq. (2), the *charges* assigned to the Schmidt states are not. Under translation, the charges of the Schmidt states on bonds $\bar{n}, \bar{n}+M$ are related by

$$\big(\overline{C}_{\overline{n}+M}, \overline{K}_{\overline{n}+M}\big) = \big(\overline{C}_{\bar{n}}, \overline{K}_{\bar{n}} + M\overline{C}_{\bar{n}} - M\langle\!\langle \overline{C} \rangle\!\rangle\big). \tag{3}$$

The value $\langle\!\langle \overline{C} \rangle\!\rangle$ is a constant of the MPS defined in the next section [Eq. (10)].

B. U(1) charge conservation for iMPS

Let $\hat{Q}_T = \sum_n \hat{Q}_n$ be an Abelian charge given by a sum of all single site terms $\hat{Q}_n$. Making a cut on bond $\bar{n}$, we can decompose $\hat{Q}_T = \sum_{n<\bar{n}} \hat{Q}_n + \sum_{n>\bar{n}} \hat{Q}_n = \hat{Q}_L + \hat{Q}_R$. For a *finite* size state $|\psi\rangle$ with a Schmidt decomposition $|\psi\rangle = \sum_\alpha \lambda_\alpha |\alpha\rangle_L |\alpha\rangle_R$ on bond $\bar{n}$, the Schmidt states must have definite charge, $\hat{Q}_L |\alpha\rangle_L = \overline{Q}_{\bar{n};\alpha} |\alpha\rangle_L$. In the MPS representation, charge conservation is expressed through the corresponding constraint [1, 2]

$$\left[\overline{Q}_{\overline{r};\beta} - \overline{Q}_{\overline{l};\alpha} - \hat{Q}_{n;j}\right] B^{[n]j}_{\alpha\beta} = 0 \tag{4}$$

where $\overline{r}/\overline{l}$ denote the bonds to the right/left of site n. Pictorially, exponentiating the constraint implies

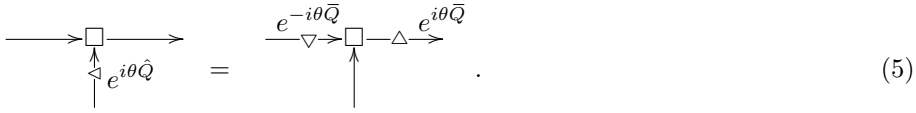

(5)

We can define a diagonal operator $\overline{Q}_{\bar{n}}$ acting on the auxiliary bonds of the MPS with diagonal entries $\overline{Q}_{\bar{n};\alpha}$. It is convenient to define a 'bond' expectation values of a $\bar{Q}_{\bar{n}}$ by

$$\langle \bar{Q}_{\bar{n}} \rangle \equiv \sum_\alpha \lambda^2_{\bar{n};\alpha} \overline{Q}_{\bar{n};\alpha} \tag{6}$$

where $\lambda_{\bar{n}}$ are the Schmidt values on the bond $\bar{n}$. In the finite case, this gives the expected charge to the left of the cut, $\langle \bar{Q}_{\bar{n}} \rangle = \langle \hat{Q}_L \rangle$.

In the case of an iMPS, the necessary and sufficient condition for the iMPS to have definite charge is again that there exist bond operators $\overline{Q}_{\bar{n}}$ such that Eq. (4) is satisfied. However, Eq. (4) is clearly invariant under a uniform shift of the bond charges, $\overline{Q}_{\bar{n}} \to \overline{Q}_{\bar{n}} + c$, so we can't obviously interpret $\overline{Q}_{\bar{n}}$ as the physical charges of the Schmidt states. This ambiguity was absent in the finite case because the left-most 'bond' at the boundary can canonically be assigned charge 0. To resolve this ambiguity, we can explicitly calculate the charge of a Schmidt state using a regulator, $Q_{\alpha L} = \lim_{\epsilon\to 0} \sum_{m<\bar{n}} e^{\epsilon m} \hat{Q}_m |\alpha\rangle_L$. Using Eq. (4) we can rewrite this charge using that auxiliary operators $\overline{Q}_{\bar{m}}$. Through an abuse of notation, we write $\overline{Q}_{\bar{m}} |\alpha\rangle_L$ as an operation on the state, by which we mean we insert $\overline{Q}_{\bar{m}}$ into the corresponding bond of the iMPS. We find

$$\begin{aligned} Q_{\alpha L} |\alpha\rangle_L &= \lim_{\epsilon\to 0} \sum_{m<\bar{n}} e^{\epsilon m} (\overline{Q}_{m+1/2} - \overline{Q}_{m-1/2}) |\alpha\rangle_L \quad \text{[Eq. (4)]} \\ &= \left[\hat{Q}_{\bar{n}} - \lim_{\epsilon\to 0} \epsilon \sum_{\bar{m}<\bar{n}} e^{\epsilon\bar{m}} \overline{Q}_{\bar{m}}\right] |\alpha\rangle_L \end{aligned} \tag{7}$$

Because $\epsilon \to 0$, the second contribution is independent of an arbitrary number of sites near the boundary $\bar{n}$. Assuming the state has finite correlation length, far from $\bar{n}$ the result becomes independent of the choice of Schmidt state α. Making use of translation invariance (assuming a unit cell of length M) and the limit $\epsilon \to 0$ we find

$$\lim_{\epsilon\to 0} \epsilon \sum_{\bar{m}<\bar{n}} e^{\epsilon \bar{m}} \overline{Q}_{\bar{m}} \left|\alpha\right\rangle_L = \frac{1}{M} \sum_{0<\bar{m}<M} \langle \overline{Q}_{\bar{m}} \rangle \left|\alpha\right\rangle_L . \tag{8}$$

where $\langle \overline{Q}_{\bar{m}} \rangle$ is again the bond expectation value of the *infinite* MPS. Hence the *physical* charge of the Schmidt state is

$$Q_{\alpha L} = \overline{Q}_{\bar{n};\alpha} - \frac{1}{M} \sum_{0<\bar{m}<M} \langle \overline{Q}_{\bar{m}} \rangle \equiv \overline{Q}_{\bar{n};\alpha} - \langle\langle \overline{Q} \rangle\rangle, \tag{9}$$

where define the $\langle\langle\rangle\rangle$ notation:

$$\langle\langle \overline{Q} \rangle\rangle \equiv \frac{1}{M} \sum_{0<\bar{m}<M} \langle \overline{Q}_{\bar{m}} \rangle . \tag{10}$$

The second term $\langle\langle \overline{Q} \rangle\rangle$ is an average of $\langle \overline{Q}_{\bar{m}} \rangle$ across the M sites of the unit cell. Using the freedom to shift $\bar{Q} \to \bar{Q} + c$, we can always cancel the second term $\langle\langle \overline{Q} \rangle\rangle$ so that $\bar{Q}$ has its 'naive' interpretation as the charge of the left Schmidt state. We will call this the 'canonical' choice of bond charges. The state has fractional charges if the required constant c is a fraction of the elementary charge.

III. NUMERICAL METHODS

In the following we explain in detail three algorithmic issues particular to FQH DMRG on an infinite cylinder: construction of the matrix product operator (MPO) for the Hamiltonian, U(1) charge conservation for the momentum K around the cylinder, and ergodicity issues of the DMRG update. The MPO formulation of iDMRG used here is explained in Refs. 3 and 4.

A. MPO representation of the FQH Hamiltonian

An MPO is a direct generalization of an MPS to the space of operators [4–6],

$$\hat{H} = \sum_{0\le\alpha_i<D} \cdots \otimes \hat{W}^{[1]}_{\alpha_1\alpha_2} \otimes \hat{W}^{[2]}_{\alpha_2\alpha_3} \otimes \cdots \quad . \tag{11}$$

Each $\hat{W}^{[n]}$ is a matrix of operators acting on site n. The dimension D of the matrices depends on the Hamiltonian, increasing as longer range components are added. For the systems studied here, $D \sim$ 100-300. An arbitrary two-body interaction in the LLL takes the form

$$\hat{H} = \sum_i \sum_{0\le m,n} U_{mn} \psi_{i+2m+n} \psi^\dagger_{i+m+n} \psi^\dagger_{i+m} \psi_i + h.c. \ni \sum_i \sum_{0<m,n}^{\Lambda} U_{mn} \psi_{i+2m+n} \psi^\dagger_{i+m+n} \psi^\dagger_{i+m} \psi_i. \tag{12}$$

To represent the MPO exactly in the limit of an infinite cylinder would require taking $D \to \infty$, but as the terms in the Hamiltonian of Eq. (12) decay like Gaussians when insertions become far apart, it is reasonable to truncate the Hamiltonian at some fixed accuracy by keeping only the largest terms. For simplicity, we will assume here a cutoff $m, n < \Lambda \sim L$.

To illustrate how to construct the MPO for Eq. (12) we view the MPO as a 'finite state machine' for constructing Hamiltonians [7]. Assuming translation invariance, to each index α of the matrix $\hat{W}_{\alpha\beta}$ we associate a state 'α' in a finite state machine, illustrated by a node in a graph. Each non-zero entry $\hat{W}_{\alpha\beta}$ is a transition probability in the finite state machine, illustrated with an edge. At the nth step, if the machine makes the transition $\beta \to \alpha$ then the operator $\hat{W}_{\alpha\beta}$ is placed at site n. The machine is non-deterministic; if there are two possible transition out of the state β, then the paths are taken in superposition, which generates the sum over all terms in the Hamiltonian.

Assuming bosons and focusing on the particular contribution highlighted in Eq. (12), at each step the MPO will place one of $\mathbb{1}$, ψ or $\psi^\dagger$. The MPO has a set of nodes which can be organized into a square grid, essentially in

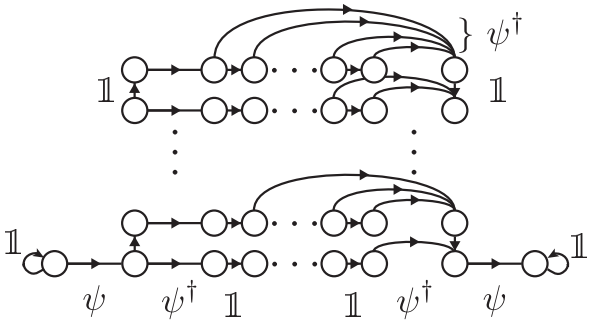

FIG. 1. Illustration of the finite state machine associated with the MPO representation of terms U_{mn} in Eq. (12). The machine begins in the node on the far left. When the first operator ψ_i is placed the machine enters the square grid. Each row of the grid corresponds to a value of m; each column, a value of n. The machine proceeds vertically up the left-most column until placing $\psi^\dagger_{i+m}$, then proceeds through row m until $\psi^\dagger_{i+m+n}$ is placed with weight U_{mn}, at which point it skips to the rightmost column. After descending down the rightmost column the final insertion ψ_{i+2m+n} is placed, at which point the term is complete and the machine remains in the terminating node to the far right. The set of all routes from the far left to far right nodes generates precisely the terms U_{mn}. A copy, with ψ and $\psi^\dagger$ swapped, also exists to generate the Hermitian conjugate, as well as terms for special cases $m, n = 0$.

correspondence with the terms U_{mn}, as explained and illustrated in Fig. 1. The rectangular nature of the graph leads to the scaling $D \sim \Lambda^2$ of the MPO. For fermions, the Jordan-Wigner string can be accounted for by replacing $\mathbb{1}$ with the string operator $(-1)^F$ where appropriate. As for an MPS, U(1) charge conservation for both number and momenta can be implemented by assigning the appropriate charges (C, K) to the D indices of the auxiliary bond.

B. Momentum conservation on an infinite cylinder

Knowing the charges transform as Eq. (3), the algorithm proceeds as follows. We store the M B-matrices of sites $n = 0, \ldots, M-1$, and keep track of the auxiliary quantum numbers on the bonds to their right, $\bar{n} = \frac{1}{2}, \frac{3}{2}, \ldots, M - \frac{1}{2}$. For updates within the unit cell, charge conservation is implemented as usual. However, for an update acting on sites 0 and $M-1$, we must 'translate' the charge data associated with site-0 to site-M using Eq. (3). After updating B, the new charge data is translated back to site 0.

C. Ergodicity of the iDMRG algorithm

The final peculiarity of applying iDMRG to the QH effect concerns the 'ergodicity' of the 2-site update. The standard iDMRG algorithm optimizes two neighboring B-matrices per step in order to avoid getting stuck in local minima of the energy landscape [3, 4, 8]. This has the added advantage that, unlike a 1-site update, the bond dimension χ can grow during the simulation. For most Hamiltonians the 2-site update is sufficient to find the optimal state, even if the initial state is taken to be a product state. However, due to the additional constraint of momentum conservation for QH, starting from some particular state it is *impossible* for the 2-site update to generate amplitude in all possible configurations. The most naive explanation is that the smallest move available to the DMRG is a 'squeeze' involving 4 sites, though this picture is not quite exact.

For the case of fermions, we have formalized and proven the following bound. Recall that because (C, K) are good quantum numbers, each Schmidt state α on bond $\bar{n}$ can be assigned a definite quantum number $(\overline{C}_{\bar{n};\alpha}, \overline{K}_{\bar{n};\alpha})$. We define a combination $\overline{P}$ of these charges by

$$\overline{P}_{\bar{n};\alpha} \equiv \overline{K}_{\bar{n};\alpha} - \frac{1}{2\nu}\overline{C}^2_{\bar{n};\alpha} - \bar{n}\overline{C}_{\bar{n};\alpha}. \qquad (\text{assume } \langle\langle \overline{C} \rangle\rangle = 0) \tag{13}$$

$\overline{P}$ has been defined so as to be invariant under translation, unlike $\overline{K}$. For the Laughlin states, which have an entanglement spectrum in one-to-one correspondence with a chiral CFT, $\overline{P}$ is precisely the total momentum of the CFT's oscillator modes [9]. Let $\{P\}$ be the set of $\overline{P}$'s present on all bonds in the MPS, and let $P_{\min}, P_{\max}$ be the minimum and maximum values they take before beginning of DMRG. We have proved that using a 2-site DMRG update $\{P\}$ always remains bounded by $P_{\min}$ and $P_{\max}$. Hence the entanglement spectrum will appear to have a momentum cutoff set by the initial state, and the 2-site update will fail to find a variationally optimal state. For

example, if we use the exact Laughlin state as the seed for DMRG (which has $P_{\min} = 0$, as the model state is purely 'squeezed'), the 2-site update will not arrive at the ground state of the Coulomb Hamiltonian, which has $P_{\min} < 0$.

Though not stated in these terms, to our knowledge this ergodicity problem was previously dealt with via two methods. One approach initialized the DMRG with a large spectrum of random initial fluctuations, and ensured by hand that the DMRG update preserves several states in each charge sector (e.g. Ref. 10). The algorithm was nevertheless observed to get stuck for several sweeps at a time, but did converge. In this approach care is required to ensure the initial state supplies adequate fluctuations $P_{\min}, P_{\max}$, and there may be additional more subtle restrictions missed by this bound. A second approach used 'density matrix corrections' (e.g. Ref. [11]), though to our knowledge there hasn't been a detailed study of whether this restores complete ergodicity.

The solution we adopt here is to generalize the DMRG to a n-site update, optimizing n sites as a time. In the MPS/MPO formulation of DMRG we implement a $2n$-site update by grouping n sites together into a single site of dimension $d = 2^n$ and then perform the usual 2-site update on these grouped sites. For $n = 2$, for example, we simply contract 2 adjacent B-matrices of the MPS, taking $B^{[0]j_0}B^{[1]j_1} \rightarrow B^{[\bar{0}]j_0 j_1}$, and likewise for the W-matrices of the MPO. As the complexity of the DMRG update scales as d^3, this does come at a cost, though it is partially offset by the increased speed of convergence. We have not seen the algorithm get stuck while using a sufficiently expanded update. Though we have not proved it, we believe that a $q+3$-site update will be ergodic for filling fractions $\frac{1}{q}, 1-\frac{1}{q}$. For more complicated fractions, such as $\frac{2}{5}$, we have checked ergodicity by trial and error; for instance, a 10-site update arrived at the same final state as a 6-site update, so the latter was used in the reported simulations.

The main advantage of previous approaches, which use a two site update, is the decreased memory required, which quickly becomes a limitation for the 6-site update when $\chi \gtrsim 4000$. Generating a random iMPS with sufficient fluctuations, conserves K, and resides in the desired topological sector is quite subtle. A more promising approach is to develop a 'density matrix correction' applicable to the MPO formulation used here.

D. Convergence with respect to truncation errors

The FQH iDMRG algorithm introduces two truncation errors; an error due to the finite number of Schmidt states kept, and an error due to the finite number of terms kept in the Hamiltonian (which is necessary for the MPO to have finite bond dimension). We refer to these as the MPS and MPO truncation errors respectively, which we address in turn.

1. MPS truncation error

The MPS ansatz implies that only a finite number of states are kept in the Schmidt decomposition, which bounds the possible overlap between the MPS and the true ground state. While the truncation relative to the exact ground state is not accessible, it is customary in iDMRG to define the 'truncation error' ϵ_{MPS} to be the weight of the Schmidt states dropped when projecting the variationally optimal $2n$-site wave function back to the desired bond dimension.

The truncation error was kept constant while the circumference L was scaled. To simulate the system at fixed truncation error, the bond dimension grows with the circumference L as [9]

$$\chi \sim b e^{vcL - d_a} \tag{14}$$

where c is the central charge of the orbital entanglement spectrum, d_a is the topological entanglement entropy, and 'v' is a non-universal number expected to vary inversely with the correlation length. b is determined by the chosen error ϵ. For the data presented in the text, $\epsilon_{\text{MPS}} = 10^{-5}$. To assess the effect of finite ϵ_{MPS} on the extracted entanglement entropy γ, we have calculated $S(L; \epsilon_{\text{MPS}})$ for $\epsilon_{\text{MPS}} = 10^{-4}, 10^{-5}, 10^{-5.5}$. The scaling of S, and the resulting estimate of γ, are reported in Fig. 2. While $\epsilon_{\text{MPS}} = 10^{-4}$ introduces spurious oscillations, the relative error in S between 10^{-5} and $10^{-5.5}$ remains about 0.2 % (while the memory requirement is multiplied by about 1.5). A similar analysis must be made on a case by case basis in order to assess the tradeoff between the reduced accuracy in S and the larger accessible L.

We note that in the most naive analysis, the truncation error contributes an error in the topological entanglement entropy, rather than the coefficient of the area law. This may be the source of the 3% error in out estimate of γ for the $\nu = \frac{2}{5}$ state. It would be worth investigating (both for FQH an other 2D DMRG studies) whether letting ϵ_{MPS} scale with the circumference might remove this error.

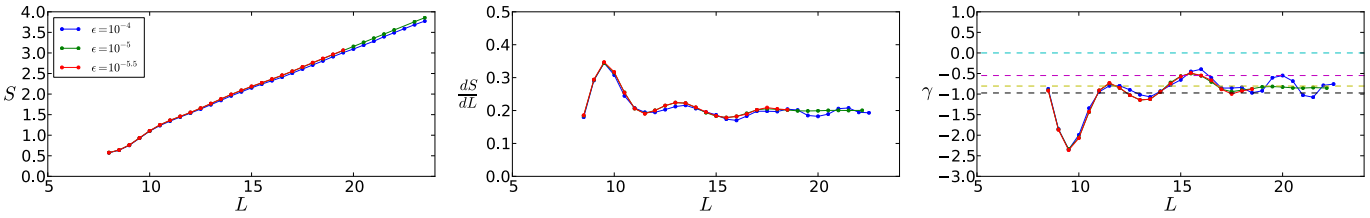

FIG. 2. Effect of finite $\epsilon_{\rm MPS}$ on S (data for $\epsilon_{\rm MPS} = 10^{-5.5}$ does not extend to $L = 23.5$). The relative error $\Delta S/S$ between different $\epsilon_{\rm MPS}$ remains bounded. While large truncation error $\epsilon_{\rm MPS} = 10^{-4}$ introduces spurious oscillations, $\epsilon_{\rm MPS} = 10^{-5}$ and $\epsilon_{\rm MPS} = 10^{-5.5}$ give the same γ to within several percent.

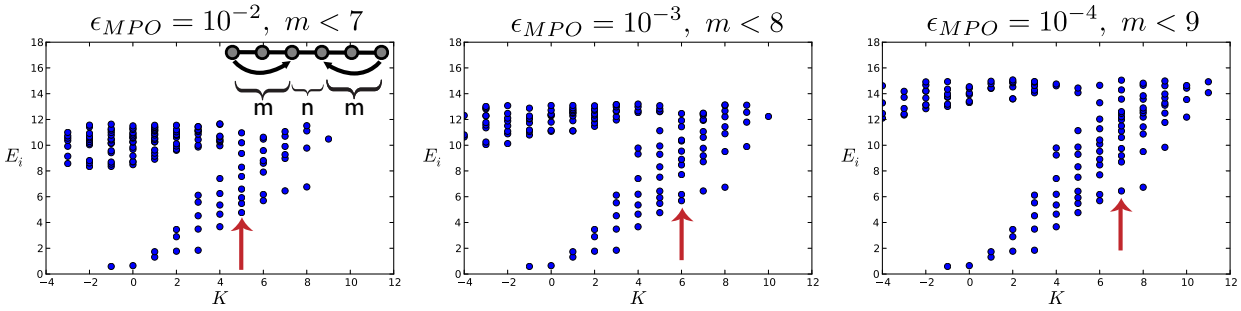

FIG. 3. Effect of finite $\epsilon_{\rm MPO}$ on the ground state entanglement spectrum of the $\nu = \frac{1}{3}$ Laughlin state at $L = 16\ell_B$. The Hamiltonian approximates the 'model' Hamiltonian V_1, but is truncated to a finite number of terms. As illustrated in the inset, this induces a cutoff in the squeezing distance $m \leq m_\Lambda$. It appears that the entanglement gap intersects the spectrum at $P_{CFT} = m_\Lambda$, as indicated by the arrows.

2. *MPO truncation error*

Truncation of the Hamiltonian to a finite range smears out the interaction along the direction y of the cylinder, but does preserve its locality. To quantify the truncation error, recall that we keep only a finite number of the V_{km} (say, the set $km \in A$), so we define the truncation error as $1 - \epsilon_{\rm MPO} = (\sum_{km\in A} |V_{km}|)/(\sum_{km} |V_{km}|)$. We hold $\epsilon_{\rm MPO} \sim 10^{-2}$-$10^{-3}$ constant as we scale the circumference of the cylinder. Because the spatial extent of this smearing is held constant as the circumference L is increased, it is as if a fixed 'cutoff' has been introduced to the Hamiltonian. When scaling $S(L) = \alpha L - \gamma$, the coefficient of the area law may modified, but the topological entanglement entropy should not be.

To illustrate the effect of the truncated Hamiltonian, we consider the model Hamiltonian for the $\nu = \frac{1}{3}$ Laughlin state. The entanglement spectrum of the model wave function is known to have identical counting as the edge CFT; by truncating the model Hamiltonian, the entanglement spectrum is modified at large momenta. As illustrated in Fig. 3, a finite 'entanglement gap' is introduced with a magnitude that increases as $\epsilon_{\rm MPO} \to 0$.

E. Obtaining the full set of minimal entangled ground states $\{|\Xi_a\rangle\}$ from iDMRG

There are two issues when constructing the MES basis. a) Does the DMRG converge to MESs, or is it favorable for it to converge to superpositions of them? b) If it does produce MES states, how do you initialize the DMRG in order to obtain all of them?

As to a), it has been shown that the MES basis is in fact the eigenstate basis on an infinite cylinder, with energy densities that have an exponentially small splitting at finite circumference L [12]. As there is no energetic reason for the DMRG to produce superpositions of the MES (and at finite χ, there is in fact a finite entanglement bias to produce MES), we expect the DMRG to produce MES.

As to b), we first consider the role of the momentum K per unit cell. The MESs are eigenstates of the momentum K: if two infinite cylinder ground states with different momenta per unit cell are added in superposition, then the entanglement entropy must increase as their Schmidt states are respectively orthogonal. The DMRG preserves K; so if the DMRG is initialized using a state in a momentum sector K that contains an MES, then the DMRG will produce an MES; if the sector does not contain an MES, the optimized energy will observed to be higher than those of sectors

that do. The first step, then, is choose an orbital configuration λ of the desired K (such as $\lambda = 010$), initialize the iDMRG with the corresponding $\chi = 1$ MPS $|\lambda\rangle_0$ by updating the iDMRG 'environments' without further optimizing the state, and then run iDMRG to obtain an optimized state and energy E_λ. Repeating for orbital configuration λ of different K, we compare the energies E_λ to determine which K sectors contain a MES, rejecting those sectors such that E_λ is not minimal within some tolerance set by the exponentially small splitting due to L.

For many of the expected phases (such at the Laughlin and hierarchy states), the ground-states are uniquely distinguished by K, so all MES will be obtained by the procedure just outlined. For certain cases, however, several of the MES have the same K, for instance those corresponding to root configurations 01110 and 10101 of the $k = 3$ Read-Rezayi (RR) phase at $\nu = \frac{3}{5}$ [13]. If we initialize the DMRG with 10101, we might worry that it will tunnel into the 01110 MES during the iDMRG, either due to the exponentially small splitting of the physical energies, or because the latter state has $d_a > 1$ and hence higher entanglement.

We argue that the iDMRG, if initialized with an approximation of one MES b, will not tunnel into a different MES a. Consider the following three energy scales: (*1*) the exponentially small, but physical, splitting between the ground-state energy per site due to the finite circumference, $E_{0;ab} = E_{0;a} - E_{0;b}$; (*2*) the difference in the DMRG truncation error per site, $E_{\chi;ab} = E_{\chi;a} - E_{\chi;b}$, which is inherent to the MPS representation. Each of $E_{0;a/b}$ can be made arbitrarily small for sufficient χ, but, at fixed χ, one of the truncation errors may be larger if $d_a \neq d_b$, as the state has higher entanglement (an effect observed for the MR state); (*3*) the gap Δ_c for inserting a quasiparticle of the type 'c' that would arise at a domain wall between the two states a, b.

If $E_{0;ab} + E_{\chi;ab} < 0$, heuristically the iDMRG may prefer to find the a state. In this scenario, if we initialize the iDMRG with the b state, it can 'tunnel' into the a state by inserting a $c, \bar{c}$ pair near the sites being updated. As the iDMRG proceeds, the state 'grows' by repeatedly inserting new sites at the center of the chain. The $c, \bar{c}$ pair then get successively pushed out to the left/right of the chain, leaving the a type GS in the central region, which the state eventually converges to. Effectively, a $c/\bar{c}$ pair has been drawn out to the edges of the 'infinite' cylinder, thus tunneling between ground-states, a problem the geometry is supposed to avoid.

However, we do not expect this to happen for energetic reasons. At a given step, the DMRG can only modify the state significantly within a correlation length ξ of the bond. Hence if a $c, \bar{c}$ pair is created, they can be drawn at most ξ sites apart during the first step. The cost to tunnel into the a state during the update is

$$E = \Delta_c - (\xi E_{0;ab} + E_{\chi;ab}) \tag{15}$$

$E_{0;ab}$ is exponentially small at large L, and E_χ should be very small if sufficient χ is used, while the quasiparticle gap Δ_c remains finite. Hence the energy of the quasiparticle provides an energetic barrier for the iDMRG to tunnel between the MESs.

If the root configurations λ are close enough to the desired MES for the purposes of the above argument, then by initializing the DMRG with different λ of the same K, the DMRG should produce the corresponding orthogonal MES. Testing successively more complicated orbitals, we can check if we have obtained a full set by summing the quantum dimensions of the states accepted thus far [12]. We have not verified if this proves to be the case for a non-trivial case such at the $k = 3$ RR state.

If the root configurations λ are *not* sufficiently close to the MES for the purposes of the above argument, it is also possible to run iDMRG while including a bias against the MES obtained so far in order to find the additional MES.

IV. QUASIPARTICLE CHARGES

In the main text we claimed that the quasiparticle charges Q_a are determined entirely by the entanglement spectrum of the iMPS $|\Xi_a\rangle$, which we demonstrate here in detail. As discussed, we suppose the MPS takes the form of $|\Xi_{\mathbb{1}}\rangle$ for $y < 0$ and $|\Xi_a\rangle$ for $y > 0$. The most general form such a state can take is

$$|a\rangle = \sum_{\alpha\beta} |\alpha\rangle_L \otimes |\alpha\beta\rangle_C |\beta\rangle_R \tag{16}$$

where $|\alpha\rangle_L$ are the left Schmidt states of $|\Xi_{\mathbb{1}}\rangle$, $|\beta\rangle_R$ are the right Schmidt states of $|\Xi_a\rangle$, and $|\alpha\beta\rangle_C$ is an arbitrary set of states in the central 'gluing' region. Without loss of generality, we suppose that the the gluing region has a length which is a multiple of q, $n = \{0, 1, \cdots, ql - 1\}$ for $l \in \mathbb{Z}$. The boundary bonds $\bar{n}_L = \bar{\mathbb{1}}$, $\bar{n}_R = \bar{a}$ are indexed by α/β respectively. Schematically, we should think of the low-lying Schmidt states on the left/right bond as being in the CFT sector $\mathcal{V}_{\mathbb{1}}/\mathcal{V}_a$ respectively.

We exploit three basic facts. First, because the central region contains a multiple of q sites, the charge C of $|\alpha\beta\rangle_C$ must be a multiple of the electron charge (which has been chosen to be 1) for all α, β. Second, the charges of the left Schmidt states are $\bar{C}_{\bar{\mathbb{1}}} - \langle\langle \bar{C} \rangle\rangle_{\mathbb{1}}$, which differ from each other only by multiples of the electron charge. Likewise, the

charges of the right Schmidt states are $-(\overline{C}_{\bar{a}} - \langle\!\langle \overline{C} \rangle\!\rangle_a)$, which differ from each other only by multiples of the electron charge. Hence the charge of the quasiparticle, Q_a, satisfies

$$e^{2\pi i Q_a} = e^{2\pi i \left[(\overline{C}_{\bar{\mathbb{1}}} - \langle\!\langle \overline{C} \rangle\!\rangle_{\mathbb{1}}) - (\overline{C}_{\bar{a}} - \langle\!\langle \overline{C} \rangle\!\rangle_a).\right]} \tag{17}$$

Again, we have taken advantage of the fact that $\overline{C}_{\bar{n}}$ is a constant modulo 1, the charge of an electron. Finally, because charge conjugation $\mathcal{C}$ acts as spatial inversion on the LLL orbitals, we must have $e^{2\pi i(\overline{C}_{\bar{\mathbb{1}}} - \langle\!\langle \overline{C} \rangle\!\rangle_{\mathbb{1}})} = 1$. As claimed,

$$e^{2\pi i Q_a} = e^{2\pi i \left(\langle\!\langle \overline{C} \rangle\!\rangle_a - \overline{C}_{\bar{a}} \right)}. \tag{18}$$

When cutting a MES on any bond, $\overline{C}$ mod 1 is single-valued, so the equation has no ambiguity.

Note that we have implicitly assumed the sector $\mathbb{1}$ appeared in the OES – but this need not be the case, as for instance in the $\nu = \frac{1}{2}$ bosonic Laughlin state. If we naively apply the above formula to $\nu = \frac{1}{2}$ Laughlin, we find particles of charge $\pm e/4$, rather than $0, e/2$. This issue is clarified using an alternate derivation of the charge via flux matrices.

V. MATRIX PRODUCT STATES ON A TORUS

Here we explain in detail the procedure to take an infinite cylinder iMPS to a torus MPS. Our approach is closely related to that of Ref. 12, but with the additional complication of having twisted boundary conditions.

A. From an infinite chain to a periodic one

We first step back and show how to convert the MPS of any gapped, infinite chain to a periodic chain, both for the trivial case when there is no 'twist,' and then in the presence of a twist generated by a symmetry. The construction in the first case, which we explain for completeness, is obvious: we cut out a segment of the iMPS and reconnect the two dangling bonds to form a ring. For simplicity in what follows we will assume bosonic chains, and introduce the correction for Fermionic chains due to the Jordan-Wigner string at a later point.

Consider two systems, an infinite chain with a unit cell of N, and a periodic chain of length N. The sites of the chains are labeled by 'n' (with $n \sim n + N$ in the periodic case). Restricting to local Hamiltonians, we can decompose $\hat{H} = \sum_n \hat{H}^{[n]}$, where each $\hat{H}^{[n]}$ is localized around site n over a length $\xi_H \ll N$ (for bosons, for example, these are the terms $\hat{H}^{[n]} = \hat{b}^\dagger_{n+1}\hat{b}_n + h.c.$, though could extend over many sites). In the infinite case, translation symmetry implies $\hat{T}^N \hat{H}^{[n]} \hat{T}^{-N} = \hat{H}^{[n+N]}$, $\hat{T}$ being the translation operator.

The energetics of the state are determined by the reduced density matrices of the system, $E = \sum_n \mathrm{Tr}(\hat{\rho}^{[n]} \hat{H}^{[n]})$. The $\hat{\rho}^{[n]}$ are reduced density matrices in a region around n large enough to include all the sites affected by $\hat{H}^{[n]}$. If the $\hat{H}^{[n]}$ of the finite and infinite chains are identical, then to find the ground state of the periodic system it will be sufficient to reproduce the local density matrices $\hat{\rho}^{[n]}$ of the infinite system. To do so, we first cut out a segment of the iMPS with two dangling bonds, $\Psi_{\alpha\beta} = B^{[0]} B^{[1]} \cdots B^{[N-1]}$, or in the pictorial representation of MPS:

$\Psi_{\alpha\beta} \;=$

. (19)

We then connect (trace over) the dangling bonds to form a ring MPS:

$\mathrm{Tr}[\Psi] \;=$

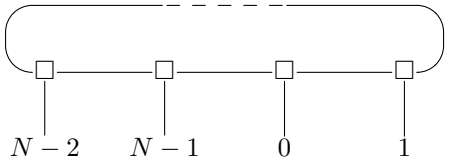

, (20)

There is no need to further optimize the MPS at the 'seam,' because when the complement to the region of $\hat{\rho}^{[n]}$ is large compared to the correlation length, $N - \xi_H \gg \xi$, then up to corrections of order $e^{-N/\xi}$ the $\hat{\rho}^{[n]}$ of the periodic MPS are identical to those of the iMPS.

1. Twists

We now introduce a twist generated by a local symmetry, $\hat{Q} = \sum_n \hat{Q}^{[n]}$, assuming each $\hat{H}^{[n]}$ is individually symmetric under $\hat{Q}$ and that $\hat{T}^N \hat{Q}^{[n]} \hat{T}^{-N} = \hat{Q}^{[n+N]}$. We use a unitary 'twist' operator $\hat{G}$ to introduce a twist every N sites of infinite chain, which generates a twisted Hamiltonian:

$$\hat{G}(\theta) = \prod_b e^{ib\theta \sum_{n=0}^{N-1} \hat{Q}^{[n+bN]}}, \qquad \hat{H}_\infty(\theta) \equiv \hat{G}(\theta) \hat{H}_\infty \hat{G}(-\theta) = \sum_n \hat{H}^{[n]}(\theta). \tag{21}$$

The chain remains translation invariant, $\hat{T}^N \hat{H}^{[n]}(\theta) \hat{T}^{-N} = \hat{H}^{[n+N]}(\theta)$, because $\hat{Q}$ is a symmetry.

We define the twisted Hamiltonian of the periodic chain to be $\hat{H}_\circ(\theta) = \sum_{n=0}^{N-1} \hat{H}^{[n]}(\theta)$ with $\hat{H}^{[n]}(\theta)$ taken from the infinite chain. In the bosonic case, for example, there is a single link with a twist, $b_0^\dagger b_{-1} e^{i\theta} + h.c.$. Note that $\hat{H}_\circ(\theta)$ is not unitarily related to $\hat{H}_\circ(0)$ except when θ is a multiple of a 'flux quantum' Φ, which we can assume is $\Phi = 2\pi$. What is the ground state $|\theta\rangle_\circ$ of $\hat{H}_\circ(\theta)$?

By construction, the Hamiltonians $H_\circ, H_\infty$ remain locally identical, so given the iMPS for $|0\rangle_\infty$, we can utilize the gluing trick of Fig. (20) already justified. As $|\theta\rangle_\infty = \hat{G}(\theta)\,|0\rangle_\infty$, with $|0\rangle_\infty$ the untwisted ground state, the desired iMPS is

$|\theta\rangle_\infty =$ 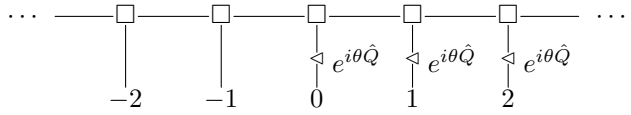

(22)

and so on throughout the chain. Using the conservation rule of (5), we can rewrite the above as

$|\theta\rangle_\infty =$ 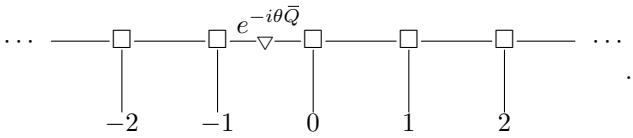

. (23)

To obtain $|\theta\rangle_\circ$, we again cut out a segment and glue,

$|\theta\rangle_\circ =$ 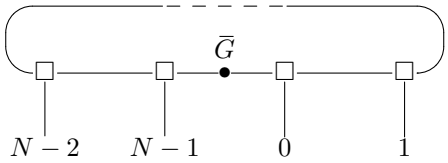

. (24)

where $\bar{G} = e^{-i\theta\bar{Q}}$.

2. Fermions

One additional modification must be made for fermions, due to the Jordan Wigner string. MPS for fermionic chains are always expressed through the occupation of bosonic operators $\sigma_n^+ = (-1)^{\sum_{j<n} \hat{N}_j} \psi_n^\dagger$, where $\hat{N}_i$ is the occupation at site i. In other words, the B matrix at site n generates the state according to $B^{j_n}(\sigma_n^+)^{j_n}\,|0\rangle$. On a periodic chain, the fermionic operators $\psi_n \sim \psi_{n+N}$ are periodic, but because of the string the σ_n^+ are not. If $\bar{N}$ is the bond operator corresponding to number, we find the string can be accounted for via

$$\bar{G} = \eta^{(N^F-1)\bar{C}} e^{-i\theta\bar{Q}}, \quad \eta = \pm \text{ for Boson/Fermion} \tag{25}$$

where N^F is the total fermion number and $\eta = \pm 1$ for bosons and fermions respectively.

In the following sections, we present the details for this construction pertaining to quantum Hall systems. First we describe the single-particle basis on an infinite cylinder by solving the Hamiltonian $H_0 = \frac{1}{2}(\mathbf{p} + \mathbf{A})^2$, then adapt the basis to a torus. We then show that in the orbital basis, the cylinder and torus Hamiltonians $H_\infty, H_\circ$, satisfy the criteria just discussed, so we can obtain the torus MPS from the cylinder MPS.

B. The cylinder geometry

Consider a cylinder finite in the x-direction with circumference L_x, infinite in the y-direction, with the following boundary condition and Hamiltonian:

$$\psi(x,y) = \psi(x-L_x,y)e^{i\Phi_x}, \tag{26}$$

$$H_0 = \frac{1}{2}(\mathbf{p}+\mathbf{A})^2, \tag{27}$$

where Φ_x is the flux threading the x-cycle and $\mathbf{p} = -i\nabla$. In the Landau gauge $\mathbf{A} = \ell_B^{-2}(-y,0)$, the x-momentum k is a conserved quantity. In that eigenbasis, the wave functions $\varphi_n^{\rm cyl}(x,y) = \langle x,y|\varphi_n^{\rm cyl}\rangle$ in the lowest Landau levels (LLL) are

$$\varphi_n^{\rm cyl}(x,y) = \frac{1}{\sqrt{L_x\ell_B\sqrt{\pi}}} e^{ik_n x} e^{-\frac{(y-y_n)^2}{2\ell_B^2}}, \qquad \text{with } k_n = n\frac{2\pi}{L_x},\ \ y_n = k_n\ell_B^2,\ \ n\in\mathbb{Z}+\frac{\Phi_x}{2\pi}. \tag{28}$$

We see that the centers of the wave functions y_n depends on Φ_x; pumping a flux through x-loop will shift all the orbitals by unit distance $\Delta y = 2\pi\ell_B^2/L_x$. Although the phases of these orbitals are arbitrary, it is convenient to resolve the ambiguity via the translation operator:

$$\hat{T}_y = \exp\left[-i\tfrac{2\pi}{L_x}\left(-i\ell_B^2\partial_y - x\right)\right], \tag{29}$$

which shifts the wavefunctions by Δy. We have chosen the phases of the orbitals such that $|\varphi_{n+1}^{\rm cyl}\rangle = \hat{T}_y\,|\varphi_n^{\rm cyl}\rangle$.

Note. We emphasize that the flux Φ_x is accounted for by labeling sites as $n \in \mathbb{Z} + \frac{\Phi_x}{2\pi}$. This carries over to the definition of the momentum: $\hat{K}_n = n\hat{C}_n$ includes the *fractional* part $\frac{\Phi_x}{2\pi}$. This definition of $\hat{K}_n$ is an important detail for the formulas that follow.

C. The torus geometry

To go from a cylinder to a torus, we identify points (x,y) with $(x-\tau_x L_x, y-L_y)$ as follows

$$\psi(x,y) = \psi(x-\tau_x L_x, y-L_y)e^{i\ell_B^{-2}L_y x + i\Phi_y}. \tag{30}$$

or equivalently $\psi(x,y) = \psi(x+\tau_x L_x, y+L_y)e^{-i\ell_B^{-2}L_y(x+\tau_x L_x)-i\Phi_y}$. The phase $i\ell_B^{-2}L_y x$ is necessary since the gauge potential $\mathbf{A}$ is not periodic when taking $y\to y+L_y$, the difference being $\mathbf{A}(x-\tau_x L_x, y-L_y) - \mathbf{A}(x,y) = \nabla(\ell_B^{-2}L_y x)$. Note that for the above to be well-defined, we need an integer number of fluxes in the torus:

$$\frac{L_x L_y}{2\pi\ell_B^2} = N_\Phi \in \mathbb{Z}. \tag{31}$$

The fluxes (Φ_x,Φ_y) parameterizes a set of Hamiltonians and corresponding Hilbert space of ground states.

To figure out the eigenstates for the torus, we sum over combinations of $\varphi_n^{\rm cyl}$ on the cylinder such that they respect the boundary condition above. The single-particle wave functions $\varphi_n(x,y) = \langle x,y|\varphi_n\rangle$ for the torus are

$$\varphi_n(x,y) = \sum_b \varphi_{n+bN_\Phi}^{\rm cyl}(x,y)\, e^{-2\pi i N_\Phi \frac{b(b-1)}{2}\tau_x - 2\pi i b n\tau_x + ib\Phi_y}. \tag{32}$$

We will use as our basis the orbitals $0\le n < N_\Phi$.

D. MPS for twisted tori

Since the flux Φ_y corresponds to a twist generated by the charge $\hat{C}$, while the modular parameter τ_x corresponds to a twist generated by the momentum operator $\hat{K}$, it is natural to suppose the orbital MPS can be obtained using a twist generated by $2\pi\tau_x\hat{K} - \Phi_y\hat{C}$. We prove this intuition is correct, but the surprise is that the ground state remains exact (up to corrections $\mathcal{O}^{-L_y/\xi}$) even though the twist is performed in *orbital* space, rather than real space.

We first determine the form of the orbital Hamiltonian of the torus, $\hat{H}_\circ(\theta)$, in the basis of Eq. (32). We assume the Hamiltonian arises from products of the electron density operators $\rho(\vec{x})$, is translation invariant in both x and y, and that any interactions, such as $\rho(\vec{x})V(\vec{x}-\vec{y})\rho(\vec{x})$, are short ranged in comparison to the length L_y of the torus. As we will eventually take $L_y \to \infty$, this is not really a restriction.

We make use of the interaction overlap integrals for the *cylinder* orbitals $\varphi^{cyl}_{n_i}$, which we denote $V_{\{n_i\}}$. The two body term, for instance, is encoded in a term $V_{n_1 n_2 n_3 n_4}$. $V_{\{n_i\}}$ is non-zero only if $\sum_i n_i = 0$, due to momentum conservation around the cylinder, and $V_{\{n_i+1\}} = V_{\{n_i\}}$ due magnetic translation invariance along the cylinder. Furthermore, $V_{\{n_i\}}$ decays when the separation between indices are such that $L_x/\ell_B \ll |n_i - n_j|$. Since $L_x/\ell_B \ll N_\Phi$, to exponentially good accuracy we can assume $V_{\{n_i\}} = 0$ if any two n_i differ by N_Φ sites.

For notational simplicity we will illustrate the calculation for the 1-body term, which generalizes in an obvious fashion. The 1-body Hamiltonian is

$$\hat{H} = \sum_{0 \le n_i < N_\Phi} \sum_{0 \le b_i \le 1} V_{n_1 + b_1 N_\Phi, n_2 + b_2 N_\Phi} e^{-f(n_1,b_1)+f(n_2,b_2)} c^\dagger_{n_1} c_{n_2} \tag{33}$$

$$f(n,b) = -2\pi i N_\Phi \frac{b(b-1)}{2}\tau_x - 2\pi i b n \tau_x + i b \Phi_y \tag{34}$$

The summand is invariant under taking all $b_i \to b_i + 1$, so we can safely restrict to terms such that $b_i \in \{0,1\}$ with at least *one* of the $b_i = 0$ (V vanishes if two indices are N_Φ apart). This leads to two types of terms: the 'bulk' terms, in which all $b_i = 0$, and the 'seam' terms, in which some $b_i = 0$ and some $b_i = 1$. The seam terms arise when site at the beginning and end of the unit cell interact.

Since $f(n,0) = 0$, in the bulk the local Hamiltonians $H^{[n]}(\theta) = H^{[n]}(0)$ are identical to the infinite cylinder Hamiltonians. Along the seam the $H^{[n]}(\theta)$ acquire phases $f(n_i,1) = -2\pi i \tau_x n_i + i\Phi_y$ for each orbital with $b_i = 1$. For example, if $N_\Phi = 10$, in the interaction $V_{9,11} c^\dagger_9 c_1 \to V_{9,11} c^\dagger_9 c_1 e^{f(1,1)}$.

Consequently the torus $\hat{\rho}^{[n]}$ should be identical to the infinite cylinder $\hat{\rho}^{[n]}$ in the bulk, but differ by phases $f(n_i,1)$ near the seam. To account for the phase $f(n_i,1) = -2\pi i \tau_x n_i + i\Phi_y$, we use the same conserved quantity manipulations as we did in Eq. (23), and find the correct twist operator $\bar{G}$ is indeed

$$\bar{G} = \eta^{(N^e-1)\bar{C}} \exp\left[-2\pi i \tau_x \overline{K} + i\Phi_y \bar{C}\right]. \tag{35}$$

$\eta = \pm 1$ accounts for bosons and fermions respectively, as discussed for Eq. (25). There is one subtlety we must emphasize: recall that $\overline{K}$ is not periodic, due to Eq. (2), so the quantum numbers $\overline{K}_\alpha$ according to the right bond of the last site and the left bond of the first site differ by $N_\Phi \bar{C}$. In the above form we assume $\overline{K}$ uses the quantum numbers according to the bond before the first site, at $\bar{n} = \frac{\Phi_x}{2\pi} - \frac{1}{2}$, *not* after the last site. The first factor $\eta^{(N^e-1)\bar{C}}$ reflects the fermion statistics among the orbitals.

VI. COMPUTATION OF FLUX AND MODULAR MATRICES VIA THE ENTANGLEMENT SPECTRUM

The flux matrices $\mathcal{F}_{x,y}$ gives the action of threading a 2π flux in the x,y-loop, while the modular $\mathcal{T}$-matrix gives the action of a Dehn twist. To derive their expression, we compute the (non-Abelian) Berry phase from the adiabatic changes $\Phi_{x,y} \to \Phi_{x,y} + 2\pi$ and $\tau_x \to \tau_x + 1$, respectively. In each case a parameter κ is varied and the Berry phase U is a $\mathfrak{m} \times \mathfrak{m}$ matrix which is a product of two pieces:

$$U = W\left(\mathcal{P} e^{i\int_{\kappa_i}^{\kappa_f} d\kappa\, A}\right), \tag{36}$$

with A and W being matrices defined as

$$A_{ab}(\kappa) = \left\langle \Xi_b(\kappa) \,\middle|\, -i\tfrac{\partial}{\partial\kappa} \,\middle|\, \Xi_a(\kappa)\right\rangle, \qquad W_{ab} = \left\langle \Xi_b(\kappa_f) \,\middle|\, \Xi_a(\kappa_i)\right\rangle. \tag{37}$$

As κ is varied, $|\Xi_a(\kappa)\rangle$ denotes the set of ground states for the boundary conditions specified by κ; A is the Berry connection and W is the overlap between the initial and final set of MES. While the result is independent of the choice of basis, in the MPS construction $|\Xi_a(\kappa_i)\rangle$ remains the MES basis.

The action of $\mathcal{F}_{x/y}, \mathcal{T}$ are characteristic of the topological phase and robust to perturbations. The results presented are summarized in Tab. I. Although the flux matrices and topological spins are formalized for a state in the torus geometry, we will show that these quantities only depend on the OES of an infinite cylinder. In particular, knowing the entanglement spectrum of each MES $|\Xi_a\rangle$ allows us to determine the charge Q_a and topological spin h_a of the quasiparticle a.

Note. There is a subtle point in the interpretation of the resulting equations. The charge Q_a and the spin h_a we will subsequently derive are those of the sector $\mathcal{H}_a$ that would arise in the real space entanglement spectra *if we were to cut the system at* $y = 0$. The entanglement spectra appearing at $y = 0$ depend on Φ_x. It is most natural to choose Φ_x such that $a = \mathbb{1}$ can appear on the cut at $y = 0$: the resulting set of 'a' are then those that would appear on the plane. We find that for fermions, this occurs for $\Phi_x = \pi$, while for bosons, this occurs for $\Phi_x = 0$. Hence it is most natural to set $\Phi_x = 0$ for bosons, and $\Phi_x = \pi$ for fermions in the following equations.

κ parameter	Berry phase matrix	Physical observable	Formula
Φ_x	$\mathcal{F}_x$	translation structure	Eq. (49)
Φ_y	$\mathcal{F}_y$	charge	Eq. (47)
τ_x	$\mathcal{T}$	topological spin, Hall viscosity, central charge	Eq. (52)

TABLE I. Summary of the non-Abelian phases from pumping Φ_x, Φ_y and τ.

A. Computing the Berry phase

We have already determined the many body state $|\Xi_a(\kappa)\rangle = \Psi^a_{j_0 j_1 \ldots}(\kappa)\,|j_0, j_1 \cdots ; \kappa\rangle$, so it is in principle a mechanical matter to calculate the Berry connection. The orbital wave function Ψ^a is given by the periodic MPS with a twist [Eq. (24)], and j_n is the occupation number of orbital φ_n defined in Eq. (32). Our approach is as follows: we first derive the general structure of the Berry phase, by decomposing the result into the 'wavefunction' and 'orbital' parts. We then report the results for the constituent terms for $\mathcal{F}_{x/y}, \mathcal{T}$.

- *A.* The connection $A_{ab}(\kappa)$ can be separated into two components, one from the changing twist in the MPS Ψ^a, and one from the changing orbitals:

$$A_{ab}(\kappa) = \sum_{\{j\}} \bar{\Psi}^a_{\{j\}}(-i\partial_\kappa)\Psi^b_{\{j\}} + \sum_{\{j\},\{k\}} \bar{\Psi}^a_{\{j\}}\Psi^b_{\{k\}}\ \langle\{j\};\kappa|\,(-i\partial_\kappa)\,|\{k\};\kappa\rangle \equiv A^{(\bar{G})}_{ab}(\kappa) + A^{(\varphi)}_{ab}(\kappa) \tag{38}$$

  The first term of Eq. (38) involves the Berry connection for Ψ^a, which depends on κ through the twist operator $\bar{G}$. In the limit of $L_y \gg \xi$, the required overlap reduces to a 'bond expectation value' as defined in Eq. (6),

$$A^{(\bar{G})}_{ab} = -i\delta_{ab}\left\langle \bar{G}^* \frac{\partial \bar{G}}{\partial \kappa} \right\rangle. \tag{39}$$

  The expectation value is taken on the bond where $\bar{G}$ sits, to the left site $n = \frac{\Phi_x}{2\pi}$. The second term of Eq. (38) involves the Berry connection between orbitals:

$$A^{(\varphi)}_{ab}(\kappa) = -i\delta_{ab}\sum_n \langle\hat{N}_n\rangle\,\langle\varphi_n|\partial_\kappa|\varphi_n\rangle\,, \quad \int_{\kappa_i}^{\kappa_f} A^{(\varphi)}_{ab}(\kappa)\,d\kappa \equiv \sum_n \theta^{(\varphi)}_n\,\langle\hat{N}_n\rangle \tag{40}$$

  where $\langle\hat{N}_n\rangle$ is the average occupation at site n.

- *W.* Likewise, the overlap W_{ab} also contains a twist and orbital component,

$$W_{ab} = \sum_{\{j\},\{k\}} \bar{\Psi}^a_{\{j\}}(\kappa_f)\,\langle\{j\};\kappa_f|\{k\};\kappa_i\rangle\,\Psi^b_{\{k\}}(\kappa_i). \tag{41}$$

  We distinguish between two cases: for $\mathcal{F}_y$ and $\mathcal{T}$, the orbitals return to themselves (), giving

$$W_{ab} = \sum_{\{j\}} \bar{\Psi}^a_{\{j\}}(\kappa_f)\Psi^b_{\{j\}}(\kappa_i) = \delta_{ab}\frac{\bar{G}|_{\kappa=\kappa_i}}{\bar{G}|_{\kappa=\kappa_f}} \quad (\text{for } \mathcal{F}_y,\, \mathcal{T}). \tag{42}$$

  For $\mathcal{F}_x$, the orbitals are translated by 1 site, and we find

$$W_{ab} = \langle\Xi_b|\hat{T}_y^{-1}|\Xi_a\rangle\,\frac{\bar{G}|_{\kappa=\kappa_i}}{\bar{G}|_{\kappa=\kappa_f}} \quad (\text{for } \mathcal{F}_x). \tag{43}$$

Because of this decomposition, the total Berry phase takes the form

$$U_{ab} = W_{ab} \exp\left[i \int A^{(\bar{G})}\right] \exp\left\langle i \sum_{\text{sites } n} \theta_n^{(\varphi)} \hat{N}_n \right\rangle, \tag{44}$$

Below we summarize the results for each case, giving an explicit formula for $\mathcal{F}_x, \mathcal{F}_y$ and $\mathcal{T}$.

1. *Orbital Berry Phase*

A technical difficulty arises when we try to compute the orbital Berry phase $\theta_n^{(\varphi)}$, due to the changing boundary conditions. To remove all ambiguity, we follow the approach of Ref. [14] by working in a coordinate system X, Y with *fixed* boundary conditions (which determines the Hilbert space) and vary the metric and gauge potential, which determines the Hamiltonian. In this approach, the boundary conditions, metric, and vector potential read

$$\tilde{\psi}(X, Y) = \tilde{\psi}(X + L_x, Y), \tag{45a}$$

$$\tilde{\psi}(X, Y) = \tilde{\psi}(X, Y + L_y)\, e^{-i\ell_B^{-2} L_y X}, \tag{45b}$$

$$\tilde{g}_{\mu\nu} = \begin{pmatrix} 1 & \frac{\tau_x}{\tau_y} \\ \frac{\tau_x}{\tau_y} & 1 + \tau_x^2/\tau_y^2 \end{pmatrix}, \quad \text{with } \tau_y = L_y/L_x, \tag{45c}$$

$$\tilde{A}_\mu = \left(\tfrac{\Phi_x}{L_x} - \ell_B^{-2} Y,\ \tfrac{\Phi_y}{L_y} + \tfrac{\pi \tau_x N_\Phi}{L_y}\right). \tag{45d}$$

The odd looking term $\frac{\pi \tau_x N_\Phi}{L_y} \in \tilde{A}_Y$ exists to counteract the $N_\Phi/2$ flux quanta inserted as τ_x increases by 1.

The coordinate system (x, y) and boundary conditions of Eq. (30) are unitarily related to (X, Y) through a change of coordinates and gauge transformation. While we omit the details of the computation, all the orbital overlaps and Berry phases can be unambiguously defined by transforming the orbitals to the (X, Y) coordinates.

We also note that under $\mathcal{T}$, examining the single particle orbitals discussed above shows that the fluxes transform as $(\Phi_x, \Phi_y) \to (\Phi_x, \Phi_y + \Phi_x)$, so U_T does not take the system back to itself unless $\Phi_x = 0$. We return to this issue when discussing modular transformations.

B. Flux matrices $\mathcal{F}_{x/y}$: quasiparticle charge and Hall conductance

- $\mathcal{F}_y$. The flux matrix $\mathcal{F}_y$ describe how the MES $|\Xi_a\rangle$ transform as a flux quanta is threaded through the y-loop. Letting $\kappa = \Phi_y$, the pieces in Eq. (44) are as follows,

$$\theta_n^{(\varphi)} = -2\pi \frac{n}{N_\Phi}, \qquad A^{(\bar{G})} = \langle \bar{C} \rangle, \qquad W_{ab} = \delta_{ab} e^{-2\pi i \bar{C}_{\bar{a}}}. \tag{46}$$

  The number operator $\hat{N}$ may be rewritten in terms of bond operators, *e.g.* $\hat{N}_n = \hat{C}_n + \nu = \bar{C}_{\overline{n+1/2}} - \bar{C}_{\overline{n-1/2}} + \nu$. With a bit of algebraic manipulation, the Berry phase can be written as

$$\mathcal{F}_y = \exp\left[2\pi i (\langle\langle \bar{C} \rangle\rangle - \bar{C}) + i\nu(\Phi_x - \pi)\right] \tag{47}$$

  We see that our formula for $\mathcal{F}_y$ is similar to that for the charge $e^{2\pi i Q_a}$ in Eq. (18). Note that $\mathcal{F}_y$ is diagonal in the basis of the MES $|\Xi_a\rangle$. Physically, this is because each quasiparticle type has a well-defined charge, modulo the electron charge. In Eq. (47) we explicitly include the Φ_x dependence, whereas in Eq. (18) we implicitly assumed $\Phi_x = \pi$, which is most natural for fermions. Since Φ_x translates the state (see below), the term $\nu\Phi_x$ encodes the Su-Schrieffer counting.

- $\mathcal{F}_x$. Inserting a flux quanta through the x-loop will in effect translate the MPS by one unit cell. We can see that the orbitals momenta, in units of $\frac{2\pi}{L_x}$, are quantized and of the form $n = \mathbb{Z} + \frac{\Phi_x}{2\pi}$, and hence as Φ_x adiabatically increases by 2π, the orbitals φ_n will evolve in to φ_{n+1}. It is easy to see that $\mathcal{F}_x$ must proportional to the translation operator $\hat{T}_y$. For $\kappa = \Phi_x$, the pieces of Eq. (44) are

$$\theta_n^{(\varphi)} = 2\pi\tau_x \frac{n}{N_\Phi}, \qquad A^{(\bar{G})} = -\tau_x \langle \bar{C} \rangle, \qquad W_{ab} = \delta_{a,b+1} e^{2\pi i \bar{C}_{\bar{a}}} \tag{48}$$

($b+1$ refers to the MES which is b translated by one site). The flux matrix takes the form

$$\mathcal{F}_x = \delta_{a,b+1}\mathcal{F}_y^{-\tau_x}\exp\left[i\nu(-\Phi_y-\pi)\right]. \tag{49}$$

In general, the flux matrices must satisfy the algebra

$$\mathcal{F}_x\mathcal{F}_y = e^{2\pi i\nu}\mathcal{F}_y\mathcal{F}_x. \tag{50}$$

C. Dehn twist $\mathcal{T}$: topological spin, central charge, and Hall viscosity

Varying $\kappa=\tau_x$ from 0 to 1, we get the Berry phase U_T. Note that under $\mathcal{T}$, the fluxes transform as $\mathcal{T}:(\Phi_x,\Phi_y)\to(\Phi_x,\Phi_y+\Phi_x)$. Thus we expect that at $\Phi_x=0$, U_T should be unambiguously defined, while at $\Phi_x=\pi$, only U_T^2 should be unambiguously defined, a point we will return to later.

For the l^{th} Landau level, the individual parts of Eq. (44) are

$$\theta_n^{(\varphi)} = 2\pi\frac{n(n-N_\Phi)}{2N_\Phi} - (2l+1)\frac{L_x}{4L_y}, \qquad A^{(\bar{G})} = -\left\langle\overline{K}\right\rangle, \qquad W_{ab} = \delta_{ab}e^{2\pi i\overline{K}_{\bar{a}}}. \tag{51}$$

(The lowest Landau level is labeled by $l=0$.) We remind the reader that for $\Phi_x\neq 0$, the site index n and $\hat{K}_n$ include a fractional part $\frac{\Phi_x}{2\pi}$, see Eq. 28. We note that the first term of $\theta_n^{(\varphi)}$ has been derived by Wen and Wang in Ref. 15. Combining them, we have

$$U_{T;ab} = \delta_{ab}\exp\left\{2\pi i\left[\overline{K} - \langle\!\langle\overline{H}\rangle\!\rangle + \frac{\nu}{2}\left(\frac{\Phi_x^2}{4\pi^2}-\frac{\Phi_x}{2\pi}+\frac{1}{6}\right) - \frac{(2l+1)\nu}{16\pi^2\ell_B^2}L_x^2\right]\right\}, \tag{52}$$

where

$$\overline{H}_{\bar{n}} = \overline{K}_{\bar{n}} - \bar{n}\overline{C}_{\bar{n}} + \bar{n}\langle\!\langle\overline{C}\rangle\!\rangle. \tag{53}$$

In light of Eq. (13) (where $\langle\!\langle\overline{C}\rangle\!\rangle=0$), we can write $\overline{H}=\overline{P}+\frac{1}{2\nu}\overline{C}^2$ and interpret $\overline{H}$ as the "energy operator" for auxiliary states. $\overline{H}$ is convenient as it is invariant under translation by q sites. As mentioned, at $\Phi_x=0$, U_T is unambiguously defined because $\overline{K}$ mod 1 is single-valued on any bond (for a MES) and so Eq. (52) is well-defined. For $\Phi_x=\pi$, however, only $\overline{K}$ mod $\frac{1}{2}$ is single-valued which implies that only U_T^2 is well-defined (cf. section on modular transformations). Finally, we also note that a term proportional to N^eN_Φ has been dropped from the result.

If we use a convention where $\langle\!\langle\overline{C}\rangle\!\rangle=0$, set $\Phi_x=\pi$ (which is most natural for fermions) and restrict to the lowest Landau level, then Eq. (52) simplifies to

$$U_{T;ab} = \exp\left\{2\pi i\left[\overline{K} - \langle\!\langle\overline{K}-\bar{n}\overline{C}_{\bar{n}}\rangle\!\rangle - \frac{\nu}{24} - \frac{\nu}{16\pi^2\ell_B^2}L_x^2\right]\right\}. \qquad \text{(When } l=0,\ \langle\!\langle\overline{C}\rangle\!\rangle=0, \text{ and } \Phi_x=\pi.) \tag{54}$$

This is the form shown in the main text.

Discussion. In order to interpret U_T, we picture the MES as a torus with a topological flux a winding around the y-cycle. We cut the torus at $y=0$, shear the segment of cylinder evenly throughout the bulk so that $y=0$ remains fixed while $y=L_y$ rotates by L_x, then reglue the ends. Since an anyonic flux a terminates at the edge, there is a quasiparticle a on the edge $y=L_y$ which moves once around the circumference under the shear. The quasiparticle has momentum $\frac{2\pi}{L_x}(h_a-c/24)$ (if the edge is not chiral, this should be understood as $h_a-\bar{h}_a-\frac{c-\bar{c}}{24}$), hence traversing a distance L_x generates a phase $e^{2\pi i(h_a-c/24)}=\theta_a e^{-2\pi ic/24}$. ($\theta_a$ is known as the 'topological spin' of the quasiparticle a.) The bulk itself shears as well, with the strain changing as $\frac{L_x}{L_y}d\tau_x$. The finite 'Hall viscosity' η_H results in a phase per unit area proportional to the changing strain [16],

$$\theta_{\text{bulk}} = \hbar^{-1}\int_{\tau_x=0}^{1}(L_xL_y)\eta_H\frac{L_x}{L_y}d\tau_x = \hbar^{-1}\eta_H L_x^2. \tag{55}$$

Together, the expected result is

$$U_{T;ab} = \delta_{ab}\exp\left[2\pi i\left(h_a - \frac{c}{24} - \frac{\eta_H}{2\pi\hbar}L_x^2\right)\right]. \tag{56}$$

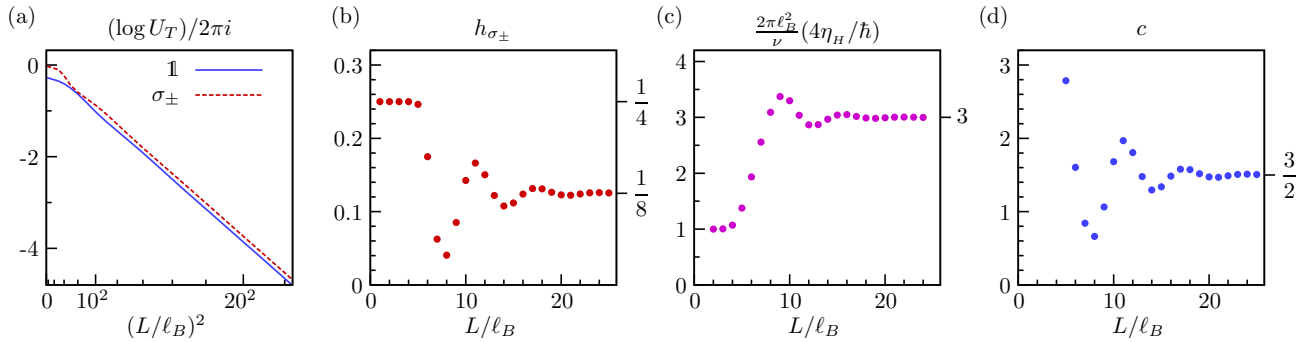

FIG. 4. Various quantities characterizing the topological Moore-Read phase at $\nu = 1/2$. The Berry phase U_T arising from a Dehn twist is acquired from the model Moore-Read wave function via Eq. (54) and h, c, η_H are extracted from Eq. (56) at various circumference $L = L_x$. (a) The argument of the phase U_T plot vs. L^2/ℓ_B^2. For large L, the argument becomes linear in L^2. (b) h of the $\sigma_\pm$ quasiparticle, extracted from the ratio of U_T between the $\sigma_\pm$ and $\mathbb{1}$ ground states, via the ratio $\exp(2\pi i h_{\sigma_\pm}) = U_T(\sigma_\pm)/U_T(\mathbb{1})$. (c) The Hall viscosity η_H extracted by fitting to the form $U_{T;\mathbb{1}\mathbb{1}} = e^{-2\pi i c/24}\exp(-\frac{\eta_H}{2\pi\hbar}L^2)$ for the identity sector. The data is presented as the 'shift' $\mathcal{S} = (2\pi\ell_B^2/\nu)(4\eta_H/\hbar)$. (d) The chiral central charge extracted from $U_{T;\mathbb{1}\mathbb{1}}$, assuming $\mathcal{S} = 3$ for the Moore-Read state. (b)-(d) In all cases L/ℓ_B must be sufficiently large for these topological quantities to be reliably extracted from the entanglement spectrum.

The Hall viscosity is known to be related to the 'shift' $\mathcal{S}$ on a sphere via $\eta_H = \frac{\hbar}{4}\frac{\nu}{2\pi\ell_B^2}\mathcal{S}$ [17]. To extract the quantities independently, we can first fit the quadratic part to extract η_H and isolate the constant part $h_a - c/24$. Once the $\mathbb{1}$ MES and bond is determined, we obtain c, and the remaining h_a's can be read off directly from the ratio $e^{2\pi i h_a} = U_{T;aa}/U_{T;\mathbb{1}\mathbb{1}}$.

In Ref. 15, the differences $h_a - h_b$ can be extracted from 'pattern of zeros,' which can be understood as the $L \to 0$ limit in which the state becomes a $\chi = 1$ tensor product. In this limit, only the term $\theta_n^{(\varphi)}$ from Eq. (51) contributes to the Berry phase U_T and hence the differences $h_a - h_b$ inferred from Eq. 52 reproduces Wen and Wang's result (Eq. (32) and (33) of Ref. [15]). However, in the limit $L \to \infty$, the ratio $\theta_a/\theta_b = e^{2\pi i(h_a - h_b)}$ computed via Eq. (52) matches that of Ref. 15 *only* when the quasiparticles a, b are related by attaching fractional fluxes (in the MES language, the states are related by translation). Hence in the (single-Landau level) Abelian case, where all MES are related by flux attachment, the spins h_a's can be recovered in the limit $L \to 0$ (using $h_{\mathbb{1}} = 0$). But for non-Abelian cases, where not all MES are related by translation, only in the $L \to \infty$ limit gives the correct result, so the result of Ref. 15 [Eq. (33)] appears to be valid only for Abelian phases.

As an example, consider the Moore-Read state at $\nu = \frac{1}{2}$. The MR state contains two non-Abelian quasiparticle 'σ_+' and 'σ_-', with charges $\pm\frac{e}{4}$ and both with quantum dimension $d_\sigma = \sqrt{2}$. Its topological spin is expected to be $h_{\sigma_\pm} = \frac{1}{2\nu}Q^2 + h_\sigma = \frac{1}{16} + \frac{1}{16} = \frac{1}{8}$. The edge of the MR phase consists of a free boson and Majorana mode with combined chiral central charge of $1 + \frac{1}{2} = \frac{3}{2}$. In Fig. 4, we plot the values of h, c and η_H extracted by fitting U_T of the model MR wavefunctions [18] to Eq. (56) at various L_x.

D. Modular transformations

The modular transformations are affine maps from the torus to itself, the set of which is the modular group $\mathrm{PSL}(2,\mathbb{Z}) \cong \mathrm{SL}(2,\mathbb{Z})/\mathbb{Z}_2$. For example, the '$T$' transformation corresponds to a Dehn twist sending $\tau \to \tau + 1$ (the same as $\tau_x \to \tau_x + 1$). The 'S' transformation rotates the torus sending $\tau \to -1/\tau$. (When $\tau_x = 0$, this corresponds to a $\pi/2$ rotation swapping L_x with L_y.) Since T and S generate the entire modular group, we focus only on these two transformations.

The $\mathcal{T}$- and $\mathcal{S}$-matrices describes how the set of ground states transform under their respective modular transformations [14]. As discussed in the previous section, $\mathcal{T}$ is a diagonal matrix with entries θ_a known as the 'topological spin', the action of rotating a quasiparticle type a by 2π. $\mathcal{S}_{ab}$ gives the mutual statistics of braiding a and b around each other. Generically $\mathcal{T}, \mathcal{S}$ are elements in a projective representation of $\mathrm{SL}(2,\mathbb{Z})$; the double cover of the modular group. The double cover is necessary because $S^2 = 1 \in \mathrm{PSL}(2,\mathbb{Z})$, but $\mathcal{S}^2$ corresponds to charge-conjugation and is not a multiple of the identity; rather $\mathcal{S}^4 \propto \mathbb{1}$.

Note that under the modular transformations the fluxes transform as $\mathcal{T} : (\Phi_x, \Phi_y) \to (\Phi_x, \Phi_y + \Phi_x)$, $\mathcal{S} : (\Phi_x, \Phi_y) \to (\Phi_y, -\Phi_x)$. As we have discussed, $\Phi_i = 0$ is most natural for bosons, but $\Phi_i = \pi$ is most natural for fermions, so we must return to this subtlety.

- Constraining (or determining) $\mathcal{S}$ from $\mathcal{F}$. When $\tau_x = 0$, we can use $\mathcal{S}$ to relate the two flux matrices [15],

$$\mathcal{F}_y = \mathcal{S}\mathcal{F}_x\mathcal{S}^{-1}. \tag{57}$$

  While this alone cannot be used to solve for $\mathcal{S}$, there are additional constraints,

$$\mathcal{S}_{\mathbb{1}a} = \frac{d_a}{\mathcal{D}} = e^{-\gamma_a}, \quad \mathcal{S}_{ab} = \mathcal{S}_{ba}, \tag{58}$$

  where d_a is the quantum dimension for the quasiparticle a, with $\mathcal{D} = \sqrt{\sum_a d_a^2}$ being the total quantum dimension. γ_a is the topological entanglement entropy for the MES $|\Xi_a\rangle$ defined in the main text. For certain phases such as the Moore-Read state and the $\nu = 2/5$ Jain state the modular $\mathcal{S}$-matrix may be determined from these constraints alone. Solving for $\mathcal{S}$ in the MES basis essentially amounts to diagonalizing $\mathcal{F}_x$.

- Flux sectors and modular transformations. A subtlety in the computing $\mathcal{T}$ and $\mathcal{S}$ is the interplay of modular transformations with boundary conditions (Φ_x, Φ_y). Since T, S change the fluxes, we need to instead consider a larger Hilbert space for which the boundary conditions may take on four possible combinations: $(\Phi_x, \Phi_y) \in \{(0,0), (0,\pi), (\pi,0), (\pi,\pi)\}$, which as a shorthand we refer to as **PP**, **PA**, **AP**, **AA**, respectively. Each of these sectors consist of $\mathfrak{m}$ linear independent ground states, for a total of $4\mathfrak{m}$-dimensional ground state manifold. The **PP** sector is closed under the action of $\mathcal{T}$ and $\mathcal{S}$, but the other three sectors mixes under modular transformations [19].

  We write $\mathcal{T}$ and $\mathcal{S}$ as block matrices, where each block is an $\mathfrak{m} \times \mathfrak{m}$ matrix describing transitions between sectors. The order of the four columns/rows are **PP**, **PA**, **AP**, **AA**.

$$\mathcal{T} = \begin{bmatrix} \mathcal{T}^{\mathbf{PP}} & & & \\ & \mathcal{T}^{\mathbf{PA}} & & \\ & & & \mathcal{T}^{+} \\ & & \mathcal{T}^{-} & \end{bmatrix}, \qquad \mathcal{S} = \begin{bmatrix} \mathcal{S}^{\mathbf{PP}} & & & \\ & & \mathcal{S}^{+} & \\ & \mathcal{S}^{-} & & \\ & & & \mathcal{S}^{\mathbf{AA}} \end{bmatrix}. \tag{59}$$

  In the minimal entangled basis, each $\mathcal{T}$-submatrix are still diagonal. In the **AP** and **AA** sectors ($\Phi_x = \pi$), the formula Eq. (52) *squared* gives the product $\mathcal{T}^+\mathcal{T}^-$, as two Dehn twists are required to come back to the same wavefunction. In other words, Eq. (52) will only give h modulo $\frac{1}{2}$.

[1] U. Schollwöck, Annals of Physics **326**, 96 (2011).
[2] S. Singh, R. N. C. Pfeifer, and G. Vidal, Phys. Rev. B **83**, 115125 (2011).
[3] I. P. McCulloch, "Infinite size density matrix renormalization group, revisited," (2008), unpublished, arXiv:0804.2509.
[4] J. A. Kjäll, M. P. Zaletel, R. S. K. Mong, J. H. Bardarson, and F. Pollmann, "The phase diagram of the anisotropic spin-2 XXZ model: an infinite system DMRG study," (2012), unpublished, arXiv:1212.6255 [cond-mat.str-el].
[5] F. Verstraete, J. J. Garcia-Ripoll, and J. I. Cirac, Phys. Rev. Lett. **93**, 207204 (2004).
[6] I. P. McCulloch, Journal of Statistical Mechanics: Theory and Experiment **2007**, P10014 (2007).
[7] G. M. Crosswhite and D. Bacon, Phys. Rev. A **78**, 012356 (2008).
[8] S. R. White, Phys. Rev. Lett. **69**, 2863 (1992).
[9] M. P. Zaletel and R. S. K. Mong, Phys. Rev. B **86**, 245305 (2012).
[10] J. Zhao, D. N. Sheng, and F. D. M. Haldane, Phys. Rev. B **83**, 195135 (2011).
[11] A. E. Feiguin, E. Rezayi, C. Nayak, and S. Das Sarma, Phys. Rev. Lett. **100**, 166803 (2008).
[12] L. Cincio and G. Vidal, Phys. Rev. Lett. **110**, 067208 (2013).
[13] N. Read and E. Rezayi, Phys. Rev. B **59**, 8084 (1999).
[14] E. Keski-Vakkuri and X.-G. Wen, International Journal of Modern Physics B **07**, 4227 (1993).
[15] X.-G. Wen and Z. Wang, Phys. Rev. B **78**, 155109 (2008).
[16] J. E. Avron, R. Seiler, and P. G. Zograf, Phys. Rev. Lett. **75**, 697 (1995).
[17] N. Read, Phys. Rev. B **79**, 045308 (2009).
[18] G. Moore and N. Read, Nuclear Physics B **360**, 362 (1991).
[19] P. H. Ginsparg, "Applied Conformal Field Theory," (1988), arXiv:hep-th/9108028.